Performance of a Newly Developed Hydrophilic Additive Blended with Different Ultrafiltration Base Polymers

Huyen T. Dang,[1] Camille Amelot,[2] Dipak Rana,[3] Roberto M. Narbaitz,[1] Takeshi Matsuura[3]

[1]Department of Civil Engineering, University of Ottawa, Ottawa K1N 6N5, Canada
[2]École Nationale Supérieure d'Ingénieurs de Limoges, Université de Limoges, 13 Rue F. Chénieux, Limoges Cedex 87031, France
[3]Department of Chemical and Biological Engineering, University of Ottawa, Ottawa K1N 6N5, Canada

ABSTRACT: The capability of modifying ultrafiltration (UF) membranes with different base-polymers using a newly synthesized hydrophilic additive was investigated in this study. Five typical base-polymers were tested: cellulose acetate (CA), polyetherimide (PEI), polyethersulfone (PES), polysulfone (PS), and polyvinylidene fluoride (PVDF). The changes in characteristics and performance of the membranes were analyzed using scanning electron microscopy (SEM), atomic force microscopy (AFM), contact angle analysis, and solute transport tests. It was found that the effect of the hydrophilic additive was different for each polymer. Higher additive contents resulted in higher permeation flux. A visible effect on water content and permeability was obtained but the impact was not shown clearly in contact angles, possibly the additive's concentration was not sufficiently high at the surface. In term of flux enhancement the PES and PVDF membranes benefited the most by the addition of the hydrophilic additive. © 2010 Wiley Periodicals, Inc. J Appl Polym Sci 116: 2205–2215, 2010

Key words: hydrophilic additive; surface modification; typical ultrafiltration based polymers; contact angles

INTRODUCTION

Currently membrane surface modification is considered as important to the membrane industry as the bulk membrane material and the membrane preparation process. The key objective is to enhance the flux and retention performance beyond the trade-off line of conventional membranes, in which high flux often leads to low retention and vice versa. The techniques applied for surface modification can be blending, grafting, coating, or exposure of the surface to radiation, plasma, ion beams, and ultrasonic waves. Among these, blending of additives into casting solutions has been studied by many researchers recently due to its simplicity and low cost approach. Only one-single-step casting procedure is required for the blended dope while for the other modification processes at least an additional processing step is necessary.[1] In the blending technique, the additives are mixed with base polymer(s) to prepare the modified membranes with different surface hydrophilicity and surface morphology. For instance, incorporation of hydrophilic polyethylene glycol (PEG) had a significant role in determining the pore size and porosity of cellulose acetate (CA) membranes, and their permeate flux and protein rejection behavior.[2] The incorporation of PEG lowered the flux reduction in the ultrafiltration (UF) treatment of machine oil-water emulsion[3] or they could act as pore reducing agents in asymmetric polyetherimide (PEI) membranes.[4] It has also resulted in higher pure water permeation (PWP) and larger pores when membranes were prepared from higher molecular weight polyethersulfone (PES).[5] However, increasing molecular weight of PEG additives (0.6, 2, 6, and 12 kD) in PS membranes led to the increase of water flux but decrease of PEG solute (12 and 35 kD) rejections.[6] Some studies have claimed that addition of certain molecular weight polyvinylpyrrolidone (PVP) to PES casting solutions resulted in better permeability while the same solute retention is maintained.[7] Sometimes it led to lower rejection.[8] The permeability and the solute retention in fact depends on type of PVP.[9] Charged additives such as sulfonated polyether ether ketone (SPEEK), or sulfonated polyether imide (SPEI), have improved the flux reduction of the PEI membranes[10–12] due to the presence of more negative charges on surface. The performance of these modified membranes, however, seems unstable. It is hypothesized that these additives may also be leached out after a long period of operation because they are all miscible in water.

In contrast to the earlier highly hydrophilic polymers, such as PEG, PVP, SPEI, or SPEEK, etc. our group has been developing surface modifying macromolecules (SMMs) for over 10 years. SMMs are prepared by the synthesis of a urethane prepolymer from a diisocyanate with a polyol, followed by end-capping with an oligomeric fluoroalcohol or PEG.[13–15] It was reported that these surface modifying macromolecules (SMMs) remained at the membrane surface for a much longer period due to the affinity between the central polyurethane (PU) segment and the host base polymer. The long chain of the PU stayed in the bulk polymer phase and end groups remained at the top selective layer surface, being in contact with air during the casting.[15] Three different types of SMMs have been developed: the hydrophobic SMMs,[1,8,13,14] hydrophilic surface modifying macromolecules (LSMMs)[15–17] and charged surface modifying macromolecules (CSMMs).[18] A key characteristic of these polymers is that they are miscible with the base (or principal) polymer, so they can readily be added into the membrane casting solution. Due to their hydrophobic or hydrophilic properties, SMMs migrate to the surface of the membrane either during the casting or the gelation process. As a result, the membrane surface becomes different from the layers below (analogous to thin-film composite membranes). SMMs have proved to impact on membrane separation processes, such as pervaporation, membrane distillation, UF, and oil/water emulsion. Studies carried out so far only investigate the effect of blending SMMs into PES.[19]

The objective of this study is therefore to investigate the effect of LSMMs blending with various host polymers on the performance of UF membranes. Five polymers (CA, PEI, PES, polysulfone (PS), and polyvinylidene fluoride (PVDF)) are selected as the base polymers to cover a wide range of hydrophilicity/phobicity spectrum. This article not only involves an evaluation of the miscibility and film formation but also assesses the migration of the SMMs to the membrane surface via contact angle measurement and water permeation tests.

EXPERIMENTS

Materials

The chemicals used in this study are listed in Table I. All polymers were dried in an oven for 2 h at 105°C and dehumidified in a dessicator. The 1-methyl-2-pyrrolidinone (NMP) was used as a solvent. The LSMM was synthesized according to the method outlined by Rana et al.[16] LSMM was synthesized by end-capping the urethane prepolymer with PEG having average molecular weight of 600 Daltons. The urethane prepolymer was formed from the reaction of methylene bis-p-phenyl isocyanate (MDI) with poly(propylene glycol) (PPG) in N,N-dimethylacetamide (DMAc) solvent (Fig. 1). The values of the n and q were calculated from the average molecular weight of PPG and of PEG, which are 7.02 and 13.23, respectively. Based on the stoichiometry of the synthesis and the M_w, the repeat unit of m and p were calculated, which are 30.57 and 15.28, respectively. Average molecular weights (weight average molecular weight, M_w, and number average molecular weight, M_n) and polydispersity index (PDI, M_w/M_n) were measured by gel permeation chromatography (GPC) (Waters Associates, Milford, MA). The polymer molecular weights were calculated using the universal calibration curve. The molecular weight characterization data of the LSMM is $M_n = 1.28 \times 10^4$, $M_w = 3.63 \times 10^4$, $PDI = 2.83$. Other base polymers data are cited in the Table I.

The T_g (glass transition temperature) was determined by differential scanning calorimeter (DSC) equipped with an universal analysis 2000 program (DSC Q1000, TA Instruments, New Castle, DE). This equipment was also used to verify the miscibility of

TABLE I
Descriptions of Chemicals

| Material descriptions	CAS number	Source	Specifications
CA (Eastman 4650, Powder)	9004-35-7	Eastman Kodak Co., Rochester, NY	Acetyl content: 40 wt %; M_w: 41 kD; PDI: 2.71; T_g: 39.7°C
PEI (Ultem 1000, natural pellet)	61128-46-9	General Electric Co., Pittsfield, MA	Specific gravity (SG): 1.27; M_w: 15 kD; T_g: 212.7°C
PES (Victrex 4100P, Powder)	25667-42-9	ICI Advanced Materials, Billingham, Cleveland, England	M_w: 31 kD; PDI: 1.55 ± 0.45; T_g: 221.4°C
PES (Ultrason E6020P, Porous Flake)	25608-63-3	BASF Aktiengesellschaft, Ludwigshafen, Germany	M_w: 58 kD; PDI: 3.6; T_g: 226.1°C; SG: 1.40
PS (Udel 3500, Pellet)	25135-51-7	Amoco Performance Products, Atlanta, GA	M_w: 37 kD; PDI: 2.11; T_g: 184.2°C; SG: 1.24
PVDF (Kynar 740, Pellet)	24937-79-9	Elf Autochem Canada, Oakville, ON, Canada	M_w: 254 kD Density (ρ): 1.78 g/cm^3; T_g: −49.4°C; T_m: 160.1°C; crystallinity: 48.3%
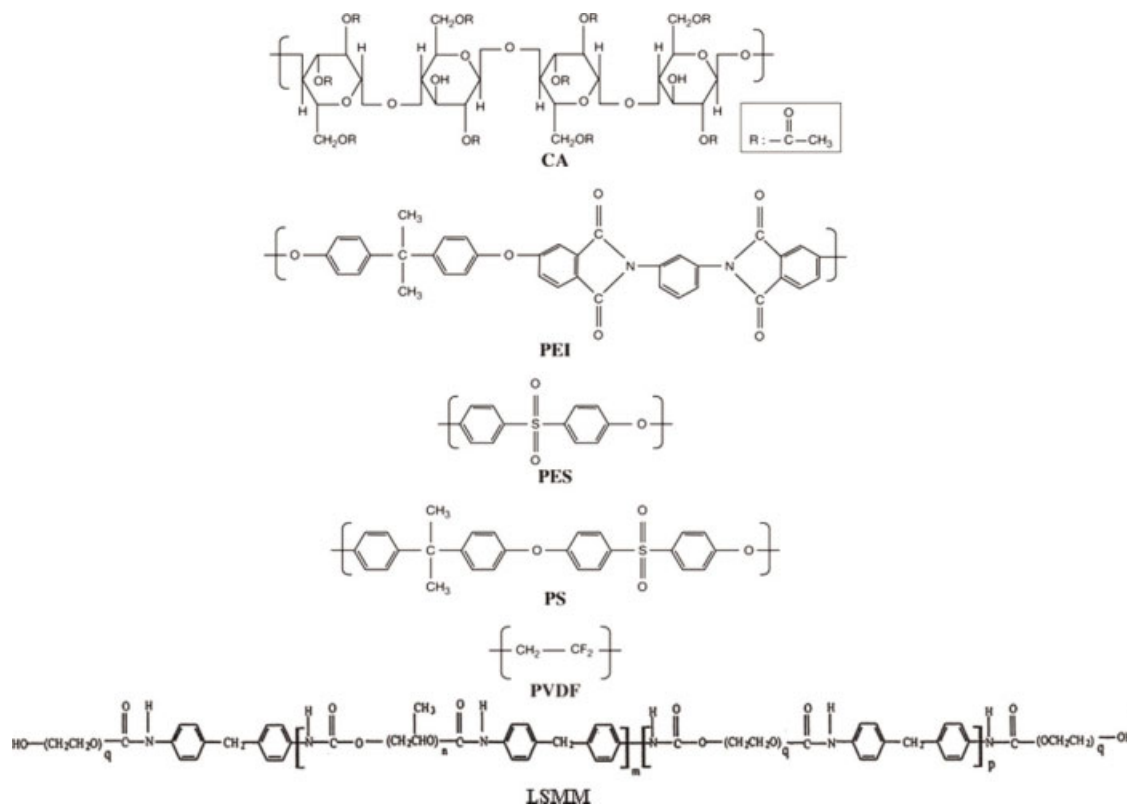
Figure 1 Chemical structures of LSMM and based polymers.

the additive LSMM in the different base polymers by evaluating T_g and T_m (melting temperature). The T_g of LSMM was 8.15°C. Reagent-grade water (MQ water) was prepared with a Milli-Q Water System (Millipore Co., Bedford, MA) which consists of activated carbon, ion exchange and organic extraction cartridges and membrane filters. Detailed chemical structures of LSMM and the base polymers are shown in Figure 1.

Membrane preparation

The membranes were prepared by the following phase inversion procedure. The casting solutions with compositions shown in Table II were prepared. Note that all casting solutions contained 18 wt % of the base polymer. The LSMM concentrations were 0.0, 0.5, and 3.0 weight percent and the balance was NMP as solvent. The three components (base polymer, LSMM, and solvent) were loaded in 250 mL bottles and mixed vigorously in an incubator orbital shaker (New Brunswick Scientific Co., Edison, N.J.) overnight at 35°C, and then stored in a dessicator for several hours to dissipate bubbles. The solutions were cast onto clean glass plates using a casting knife with a 0.2 mm gate opening. The glass plates with the nascent membranes were immediately immersed into 4°C MQ water until they hardened. The membranes were stored in MQ water and

placed in a refrigerator until they were used. It is worth noting that all the membranes were prepared under the conditions, which yielded good PES membranes.[17,19] These composition was 18 wt % PES + up to 4.5 wt % LSMM with remainder being solvent, and the conditions were zero migration or evaporation time and gelation in a 4°C water bath. The

TABLE II
Composition of the Casting Solutions for Membrane Preparation

Sample	Base Polymer (%)	LSMM (%)	NMP (%)
PVDF-0	18	0.0	82.0
PVDF-0.5	18	0.5	81.5
PVDF-3.0	18	3.0	79.0
PS-0	18	0.0	82.0
PS-0.5	18	0.5	81.5
PS-3.0	18	3.0	79.0
PEI-0	18	0.0	82.0
PEI-0.5	18	0.5	81.5
PEI-3.0	18	3.0	79.0
CA-0	18	0.0	82.0
CA-0.5	18	0.5	81.5
CA-3.0	18	3.0	79.0
PES-58-0	18	0.0	82.0
PES-58-0.5	18	0.5	81.5
PES-58-3.0	18	3.0	79.0
PES-31-0	18	0.0	82.0
PES-31-0.5	18	0.5	81.5
PES-31-3.0	18	3.0	79.0

permeation test for those membranes was described in detail elsewhere.[19]

Contact angle (CA) measurement

The membrane samples were cut into 5 × 25 mm pieces and fixed onto 25 × 75 × 1 mm superfrost micro slides (VWR, Mississauga, ON) using electrical tape. Advancing contact angles were determined using VCA Optima Surface Analysis System (AST Products, Billerica, MA). They are recorded as the critical angles, at which the edge of contact between water drop and membrane expands. The water drop volume ranged from 2.5 to 3.0 μL. The reported contact angles are the average of 10 measurements.

Water content

Water content defined by equation[1] was determined by gravimetric analysis.

$$W_\% = \frac{W_{wet} - W_{dry}}{W_{wet}} \times 100 \qquad (1)$$

where, W_{wet} and W_{dry} are mass (g) of the wet and dry membranes, respectively. The membranes were dried by keeping them in an oven at 75°C for two days.[20] The membrane samples and trays were weighed before (W_{wet}) and after drying (W_{dry}). Three measurements were conducted for each membrane type and the average values were reported.

Morphology and porosity

Membranes' morphology was examined via atomic force microscopy (AFM) and scanning electronic microscopy (SEM). A Nanosurf® easyScan 2 atomic force microscope (AFM) equipped with a software (version 1.3, Nanosurf AG, Grammmmetstrasse, Liestal, Switzerland) was used for characterization of samples. The average surface roughness (R_a) in an area of 2.52×10^{-11} m^2 was calculated for the top membrane surface via the AFM's software calculation. A model JSM-6400 JEOL (Japan Electron Optics, Japan) SEM was employed to observe the cross-sectional area of the dry membranes. Pore property and

molecular weight cut-off (MWCO) were obtained through the solute transport method.[21]

RESULTS AND DISCUSSION

Miscibility

The LSMM was visually miscible in all the tested polymer solutions. The casting solutions had different appearances for the various base polymers (Table III). There were no distinguishable differences between the solutions, as well as the membranes, of the same base polymer with and without LSMMs. Solutions with the lower LSMM concentration (0.5 wt %) were easier to cast. Whereas incorporation of a greater amount of LSMM (3.0 wt %) made the formation of membranes with good appearances more difficult, especially for those with CA and PVDF as base polymers. It seems that the miscibility of LSMM in the latter polymers was lower at a higher LSMM content. Their solutions were less viscous and not completely homogeneous. Nevertheless, with the same 0.5 wt % LSMM content, the viscosity range was PVDF < PES < PS < PEI < CA. The CA-based membranes were fragile compared with the others.

As stated earlier, to further verify the miscibility of the additive in the different base polymers, DSC analysis was performed for solid membrane samples. The DSC analysis showed that the amorphous LSMM mixed well with the amorphous base polymers, such as PEI and PES, as the blended membranes had only a single transition (Fig. 2). The T_g of the LSMM blended polymeric membranes were lower than that of the corresponding base polymer (Table I), which indicated that these systems were partially miscible at the molecular scale. It is worth noting that as the LSMM concentration increased, the T_g decreased. For example, the T_g values of 0.5 and 3 wt % of LSMM blended PES-58K membrane were 213.71 and 202.8°C, respectively. Similarly, the T_g values of 0.5 and 3.0 wt % of LSMM blended PEI membrane were 199.34 and 158.68°C, respectively. Given the lower T_g values PES appears to interact more strongly with LSMM at the 3 wt % level. In contrast, for the case of LSMM blended PVDF membranes, double melting peaks were observed (Fig. 2).

TABLE III
Solution and Membrane Appearances

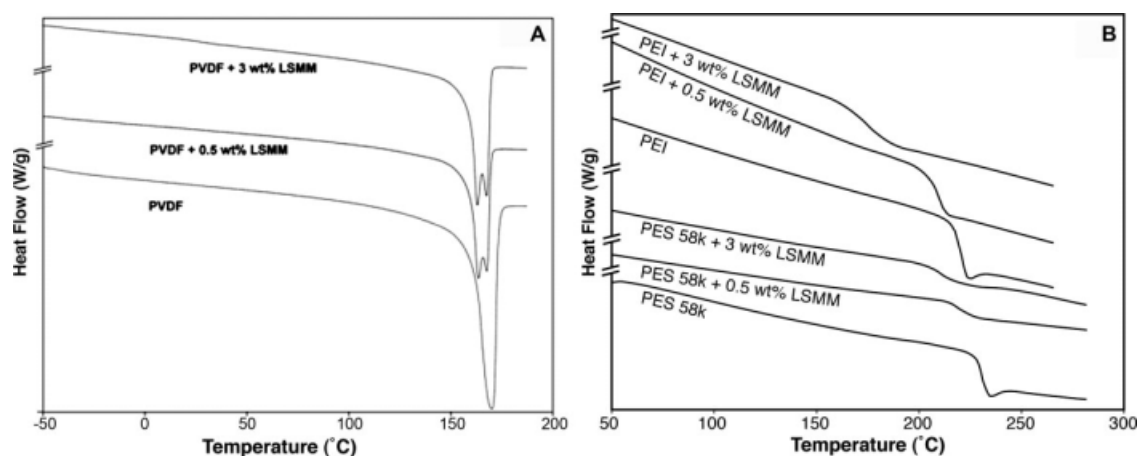| Polymer	Solution appearance	Membrane appearance
PS	Clear yellow and viscous	White and rigid
PEI	Dark yellow and viscous	Beige and flexible
PES58k and PES31k	Clear yellow and fluid	White and a bit wrinkly
CA	Transparent and viscous	Transparent and rubbery
PVDF	Transparent and fluid	Transparent and very flexible

Figure 2 DSC response for (A) crystalline PVDF membranes with/without LSMM; (B) amorphous PEI and PES 58k membranes with/without LSMM.

The melting maximum peaks were 163.9 and 168.0°C for 0.5 wt % LSMM blended PVDF, however, 163.5 and 167.9°C for 3.0 wt % LSMM blended PVDF membrane. This data reflected that LSMM influenced the crystallization of the PVDF chain segments as PVDF is a crystalline polymer in nature in contrast to the amorphous base polymers discussed earlier. Accordingly, two different kinds of lamellae were formed. One peak represented the pure PVDF chain segments, and the other peak was the representation of the PVDF chain segments contaminated with LSMM chain segments. The response of CA-LSMM was similar to PVDF (not shown in here). While this indicates that the PVDF-LSMM and CA-LSMM membranes are likely to be ineffective, the DSC data did not become available until the filtration test was completed. Therefore, the performance and characteristics of all blended membranes including CA and PVDF based were evaluated and reported later.

Molecular weight cut-off (MWCO)

The MWCOs of the membranes determined by UF experiments with PEGs and PEO as the solutes are shown in Figure 3. With the addition of LSMM, the MWCOs were altered in different ways depending on the base polymers. In almost all cases, however, the addition of LSMM increased the MWCOs, except for PES58k membranes where an increase in LSMM concentration from 0.5 to 3.0 wt % resulted in a smaller MWCO value.

The order in membrane MWCO is CA < PEI < PS < PES < PVDF, when LSMM is not blended. For convenience, polymers are classified into the following three groups to explain not only the MWCO data but also some other experimental results obtained in this work: (1) CA contains alicyclic and polar functional groups; (2) PES, PEI, and PS with

intermediate MW, containing aromatic and some polar functional groups; and (3) PVDF with the highest MW, containing straight an aliphatic chain and highly nonpolarizable fluorine. From the MWCO data, it is observed that MWCO increases progressively from the first to the third group of the polymers. This is consistent with the fact that CA is a polymer used for manufacturing many commercial reverse osmosis (RO) and nanofiltration (NF) membranes while PVDF is a polymer for many commercial MF membranes. Of course this trend can not be generalized as the performance of the membranes depends on many other factors involved in the membrane preparation.

The MWCO of CA and PEI were small compared with those reported in the literature.[10,22] It is suspected that the discrepancy is due to the membrane preparation conditions used in this study, which differ from the standard ones for CA and PEI membranes. In this study, the base polymers were dissolved solely in NMP solvent to limit the variability in comparison. However, higher MWCO of CA membranes (i.e., 40–50 kD) could be obtained if CA was mixed in acetone/dioxin/tetrahydrofuran (THF)/DMAc/dimethyl-formamide (DMF).[21] Likewise, for PEI membranes, Bowen et al.[10] observed that the membrane pore sizes increased from undistinguishable to 3 nm when the solvent changed from NMP to dioxan/THF. Thus, solvents other than NMP would likely produce better for CA or PEI membranes.

Figure 3 also shows that PES molecular weights have a significant impact. Theoretically, with the same weight concentration, the polymer with a higher MW will become less viscous and slower demixing will occur, leading to a denser membrane with a lower MWCO. This expectation was not only confirmed by this experimental data but also by some previous studies.[23]
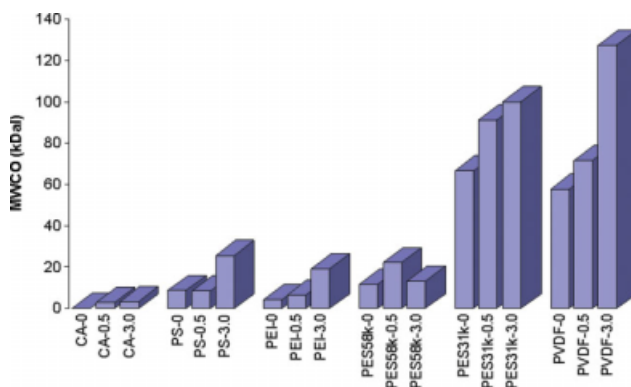
Figure 3 MWCO of membranes. [Color figure can be viewed in the online issue, which is available at www.interscience.wiley.com.]

Water content and hydrophobicity

Before the contact angle measurements, all the membranes were subjected to drying. Three methods of drying were compared: drying after solvent exchange with ethanol, drying in an oven at 75°C and natural drying in ambient air. The contact angles obtained by the aforementioned three methods did not show any statistically significant differences (Fig. 4). Hence, natural air drying was adopted.

The contact angle data shown in Figure 4 are for four polymeric materials and for different LSMM concentrations. Compared with the contact angle data that were obtained for the control dense films (without additives) i.e., PES ($\sim$ 75°), PVDF($\sim$ 83°),[24]

PEI ($\sim$ 86°),[25] PS ($\sim$ 80°),[26] the above contact angles are lower without exception. This is because the membranes studied in this work are porous and the water in the membrane pores brought down the contact angle values. Another observation can be made is that blending LSMM did not change the contact angle significantly regardless of the amount of LSMM added. Rana et al.[16] and Nguyen et al.[17] both reported that the addition of LSMM only marginally changed the contact angles of PES membranes. Thus, the noticeable changes observed in MWCO are not due to the change in the contact angle. The contact angles did not change as a function of additive contents; however, they may do if time for migration (before gelation) is incorporated.

Figure 5 shows that the water content is correlated to the contact angle. As the contact angle decreases the water content increases. This follows the natural behavior as both (contact angle decrease and water content increase) are an indication of an increase in hydrophilicity. Considering further that the contact angle is related to the surface, while the water content is a bulk property, the earlier correlation implies that the surface property is affected by the bulk property and vice versa. This is logical considering that the contact angle also depends also on the presence of water in the membrane pores and hence on the morphology underneath the top surface layer. The correlation, however, is not strong statistically, when considering the narrow range of change in water content.
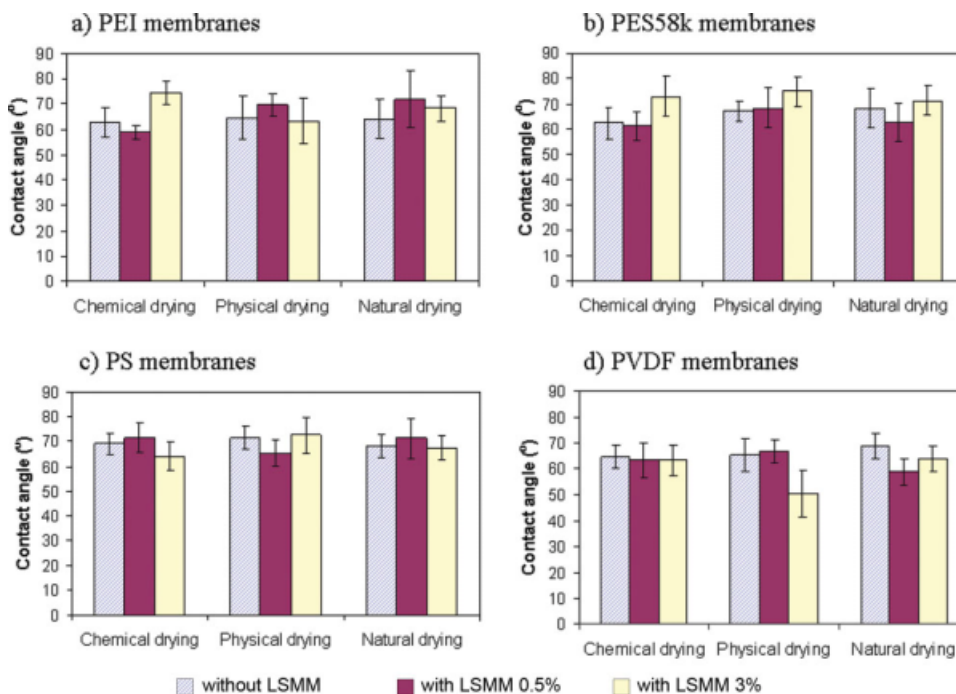

Figure 4 Advancing contact angle for each polymer as a function of the different drying methods. [Color figure can be viewed in the online issue, which is available at www.interscience.wiley.com.]
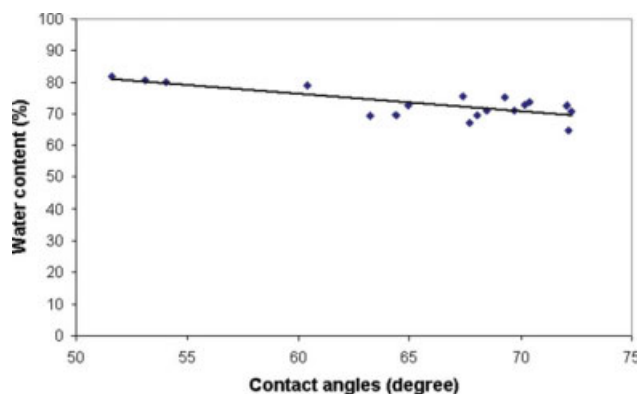
Figure 5 Correlation plot between water content and contact angles. [Color figure can be viewed in the online issue, which is available at www.interscience.wiley.com.]

Water permeation

The PWP flux is given as a function of the operation period for the six membrane samples that do not contain LSMM (Fig. 6).

Note that the flux decreases with time, which is the result of the membrane compaction. The order in the pure permeation rate is CA < (PS < PEI < PES) > PVDF. Again classifying the polymers into the groups (CA), (PES, PEI, and PS) and (PVDF) with progressively increasing hydrophilicity, the permeation rate of the membrane from the first group (CA) is lower than those of the membranes belonging to the second group. This is understandable as the MWCO of the membrane from first group (CA) is lower than the second group. Interestingly, the permeation rate of the third group (PVDF) is lower than the second group despite the fact that the PVDF membrane showed the largest MWCO. This seems to be due to the higher hydrophobicity of PVDF. Penetration of water into the smaller pores is prevented by the hydrophobic property of PVDF and only large pores are open to water flow, resulting in a high MWCO value and a low permeation rate. It should be noted that all the membranes were prepared under the same conditions (concentrations of casting solution and casting procedure). To produce optimal membranes with other base polymers may require other casting solution compositions and/or casting conditions.

The change of flux due to the incorporation of LSMM in the casting solutions is presented in Figure 7, where the % flux change is defined by the following equation.

$$\% \text{ Flux change} = \frac{J_{\text{withLSMM}} - J_{\text{withoutLSMM}}}{J_{\text{withoutLSMM}}} \times 100 \quad (2)$$

whereas J_{withLSMM} (l/m^2/h) and $J_{\text{withoutLSMM}}$ (l/m^2/h) are the pure water fluxes corresponding to the membranes prepared from the same host polymer with and without LSMM blending. The figure shows

the change of the parameter given earlier as a function of operating time. The positive percentage of flux change illustrates an increase in the pure water flux by SMM blending. Furthermore, the line slopes indicate the effect of SMM blending on the membrane compaction, i.e., the upward trend indicates less compaction, horizontal line equal compaction, and downward trend the stronger compaction of the membranes in which LSMM is blended.

The following observations can be made.

1. Lines for the % flux change are always above zero except for the case of base polymer PES58k and 0.5 wt % LSMM.
2. The % flux change increases as LSMM concentration increases from 0.5 to 3.0 wt %.
3. The three groups (CA), (PES, PEI, and PS) and (PVDF) were impacted differently. The effect of SMM blending is the weakest for the first group with an average of 12% flux increase, followed by the second group with an average of 65% and further by the third group with an average of 160%. PES58k is the exception with its small gain in the pure water flux by LSMM blending. This may be due to the high molecular weight of the polymer that makes the membrane more rigid and resistant to the pore expansion. In contrast, the LSMM additions to CA membranes only resulted in limited flux improvements. Again, the reason might be due to the nonoptimal solvent and concentration of components in casting solution. If cellulose nitrate/acetate polymer was dissolved in acetone and added with 12% glycerol[27] or 20% PVP,[28] PWP rates would have been higher.
4. Except for a very obvious downward trend of PVDF with 3.0 wt % LSMM, the lines are mostly horizontal. Interestingly, there are two cases of upward trend, i.e., PS with 0.5 wt % LSMM and PES58k with 3 wt % LSMM. This means the compaction of the membranes with
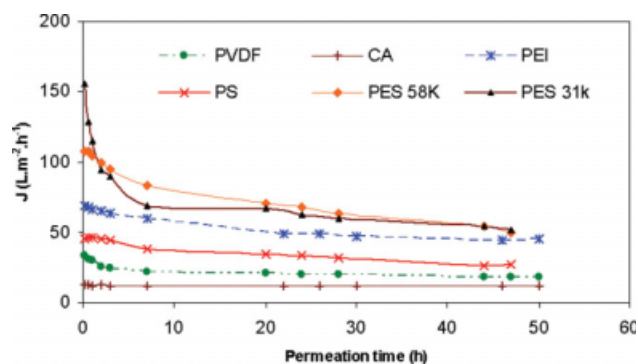

Figure 6 Pure water permeation flux of membrane with no addition of LSMM. [Color figure can be viewed in the online issue, which is available at www.interscience.wiley.com.]
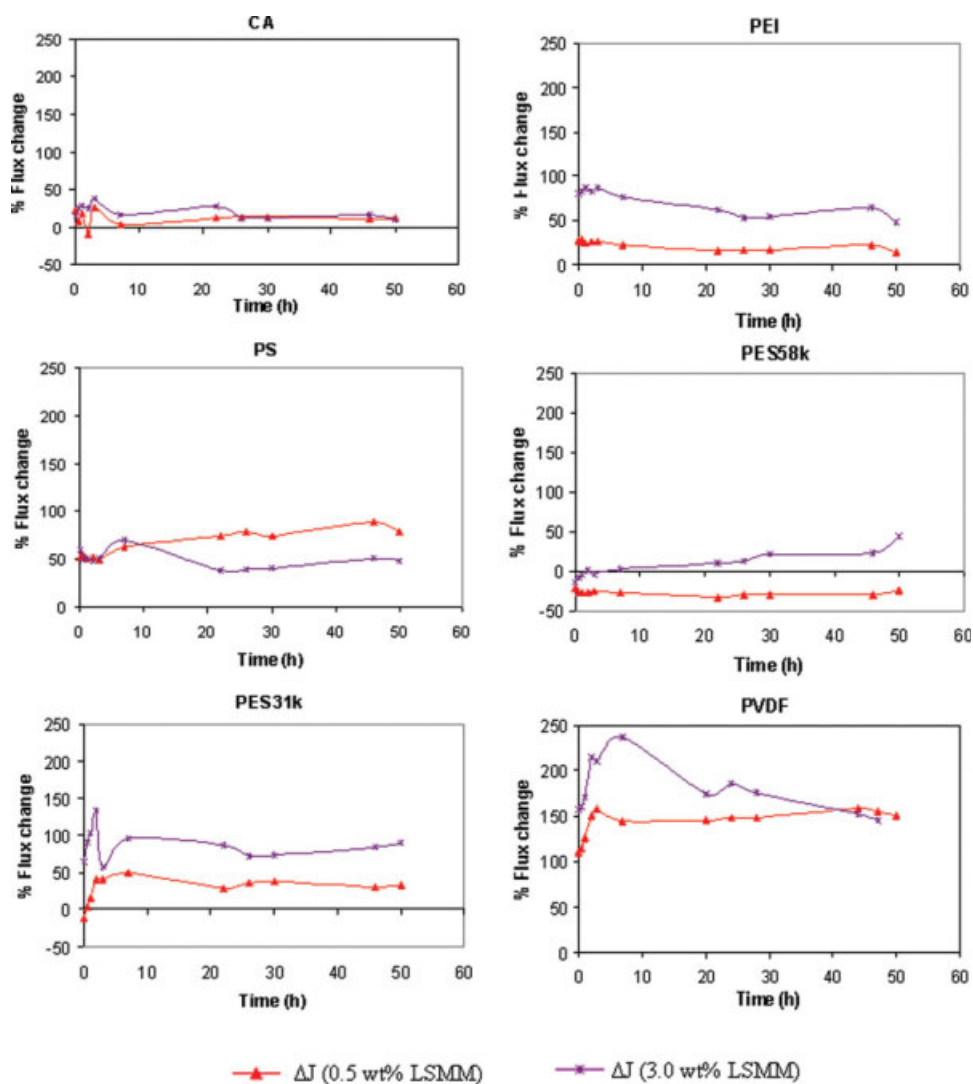
Figure 7 Percent of flux change as a function of filtration time. [Color figure can be viewed in the online issue, which is available at www.interscience.wiley.com.]

LSMM blending is equal to or less than the membrane without LSMM blending despite the increase in the pore size. Usually, compaction becomes more severe with an increase in the pore size when the membranes are prepared from the same polymeric material. Therefore, it can be concluded from the results, LSMM blending made the membranes mechanically stronger. Increase in mechanical strength of the membrane by blending a hydrophobic SMM was reported earlier.[1]

The behavior of different membranes with 3 wt % LSMM are further illustrated in Figure 8, indicating the relationship between the water flux and transmembrane pressure. The CA-based membranes were not included in this figure due to very low fluxes at low pressures. A steep slope indicates the high permeability under the increasing compression (com-
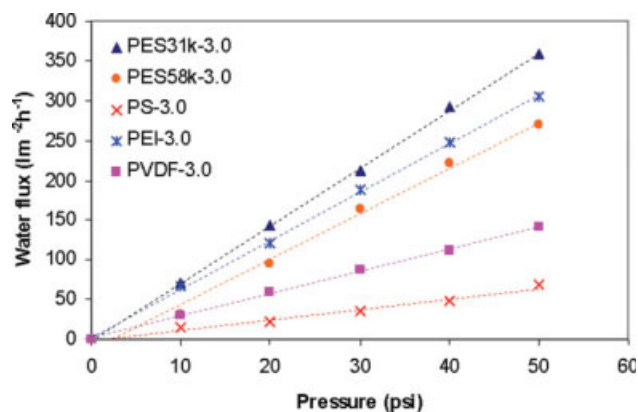

Figure 8 Relationship of water flux w.r.t transmembrane pressure. [Color figure can be viewed in the online issue, which is available at www.interscience.wiley.com.]
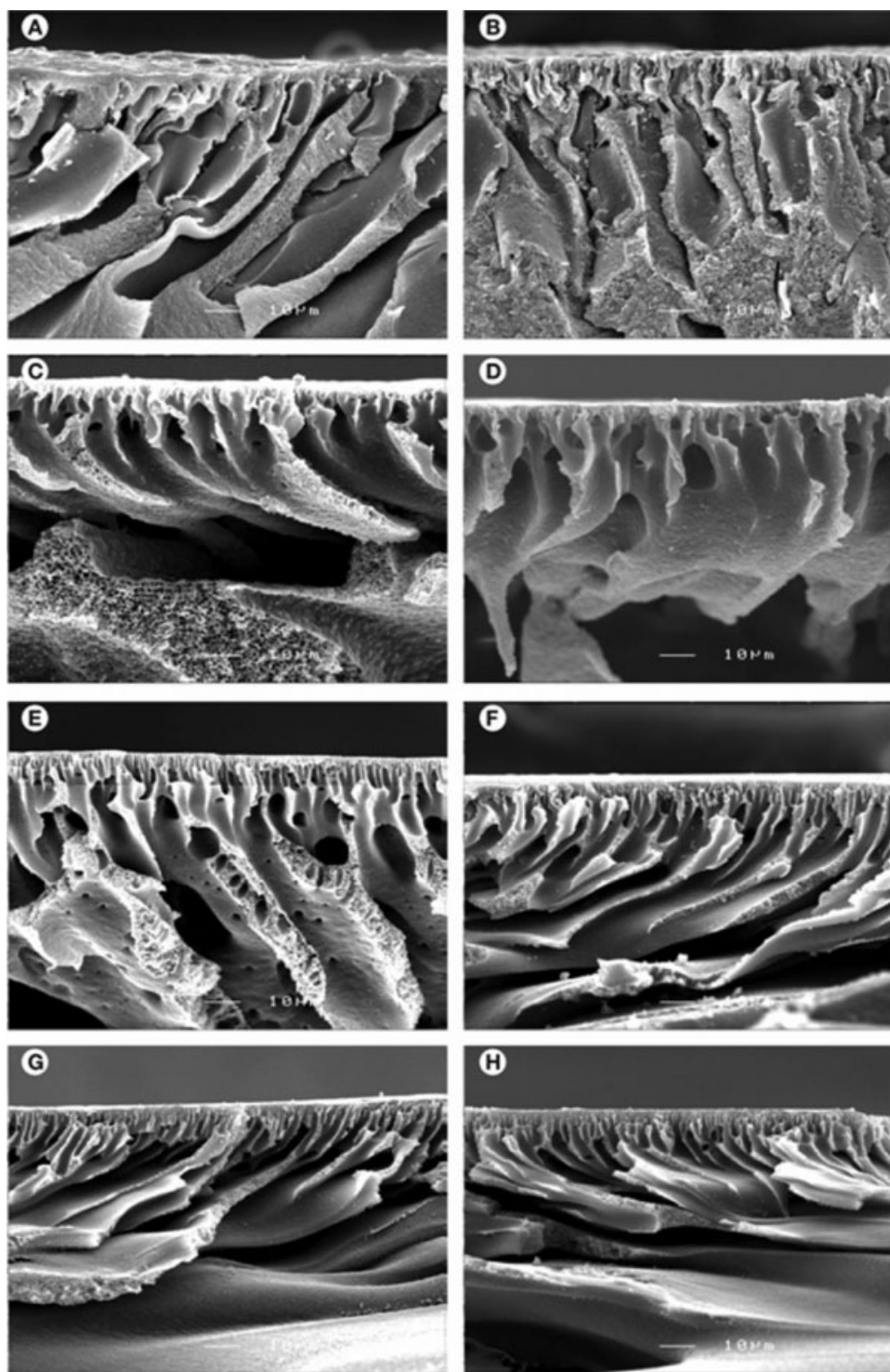
Figure 9 SEM photographs of the cross section surface of the membranes: (A) CA; (B) CA–3.0; (C) PVDF; (D) PVDF-3.0; (E) PES31k; (F) PES31k-3.0; (G) PES58k; (H) PES58k-3.0.

paction). PES31k apparently had the highest fluxes at any operation pressure. Comparing the water flux of the unmodified membranes (Fig. 6) and the modified membranes (Fig. 7), the order of the permeability among membranes was almost the same except for the PES31k and PES58k. Certainly, though all the fluxes were increased with the addition of the hydro-

philic additive, PES31k and PVDF membranes nevertheless were proved to benefit most from the addition.

SEM images and roughness

This last section would further elucidate the impact of LSMM additives via SEM images and AFM

TABLE IV
Membrane Surface Roughness

Membrane	Control (nm)	+0.5 wt % LSMM (nm)	+3 wt % LSMM (nm)
CA	0.67	10.54	13.37
PEI	2.40	1.72	2.26
PS	1.05	3.04	2.39
PES58k	0.89	1.05	1.10
PES31k	1.27	1.56	2.73
PVDF	4.32	3.46	1.64

information. Figure 9 presents the cross-sectional views of membrane surfaces with LSMM (B, D, F, H) and without LSMM (A, C, E, G). A typical asymmetrical structure consisting of a dense top layer and a finger-like porous sub-layer can be seen in most cases due to the strong affinity between NMP (used as a solvent) and water (as a coagulant).[29] However, the distance from the top surface to the end of macro voids became shorter for CA membranes with additives, while it was larger for PVDF-3.0 membranes. For PES-58k membranes, no significant change was observed. It could be explained based on the modifying capacity of polymers, especially through their chemical structures in Figure 1. The PVDF polymer has a simpler structure, whereas the complexity in structures increases from PES to PEI and CA polymers with increasing aromatic rings. Usually the presence of aromatic or heterocyclic groups reduces the rotation of the main chain, affecting the number of possible interaction sites between the various chains.[22] Therefore, the morphologic alteration showed clearer in cases of PVDF and PES-31k membranes in a way of being more porous. The changes of morphology may result in the changes of fluxes,[30] which could be seen in the Figure 7.

The surface morphology in terms of roughness (R_a) would be described in Table IV. The additive might interact differently with different base polymers affecting the casting solution properties and the resulting membranes, however, how it impacts the membrane surface roughness is unclear. Apparently, the trend of roughness variation followed the classification: (i) Roughness of the control membranes increased gradually from Group 1 to Group 3; (ii) Group 1 (CA) roughness increased significantly (with the factor >15); (iii) Roughness of the Group 2 (PEI, PS, and PES) membranes remained almost stable (with the factor around 2) and (iv) the roughness of the Group 3 (PVDF) membrane decreased notably by LSMM addition.

The incorporation of LSMM smoothened PVDF membranes but roughened the CA membranes. Relating to the cross-section images for those membranes (CA and PVDF), the alterations of morphol-

ogy could also be seen in the first four pictures A, B, C, and D. The impact of roughness on water permeation and fouling depends on many factors involved, such as casting solutions, casting method, gelation process, and post treatment if any.

CONCLUSIONS

The impact of LSMM additions to five typical UF-base polymers PS, PES, CA, PEI, and PVDF has been evaluated.

1. Based on DSC analysis, LSMM did not mix well with CA and PVDF, particularly at the higher LSMM concentration. For the other polymers, which were amorphous polymers like LSMM, the casting solutions were homogenous and easy to cast.
2. The LSMM addition under the membrane making conditions, which were not optimized for the specific base polymers, did not cause a statistically significant change in contact angle. Alternative manufacturing conditions such as increasing the migration time or introducing stronger LSMM may lead to a greater impact.
3. LSMM had a visible effect on MWCO, morphology and permeability. Statistical analysis showed that membranes' responsive characteristics and performance all depended on the types of base polymers and additions of LSMM, however, the first one played more important roles in those changes. Among the modified membranes, PES and PVDF membranes apparently had benefit from this hydrophilic additive with high flux changes or water production.
4. Different methods of drying membranes for contact angle measurements produced statistically the same readings, hence using the natural method is the best choice, which is easiest and cheapest.

References

1. Suk, D. E.; Chowdhury, G.; Matsuura, T.; Narbaitz, R. M.; Santerre, P.; Pleizier, G.; Deslandes, Y. Macromolecules 2002, 35, 3017.
2. Arthanareeswaran, G.; Thanikaivelan, P.; Srinivasn, K.; Mohan, D.; Rajendran, M. Eur Polym J 2004, 40, 2153.
3. Li, H.-J.; Cao, Y.-M.; Qin, J.-J.; Jie, X.-M.; Wang, T.-H.; Liu, J.-H.; Yuan, Q. J Membr Sci 2006, 279, 328.
4. Kim, I. C.; Lee, K. H. J Membr Sci 2004, 230, 183.
5. Idris, A.; Zain, N. M.; Noordin, M. Y. Desalination 2007, 203, 324.
6. Kim, J. H.; Lee, K. H. J Membr Sci 1998, 138, 153.
7. Ochoa, N. A.; Masuelli, M.; Marchese, J. J Membr Sci 2006, 278, 457.

8. Mosqueda-Jimenez, D. B.; Narbaitz, R. M.; Matsuura, T. Sep Purif Technol 2004, 37, 51.
9. Yang, Q.; Chung, T. S.; Weber, M. J Membr Sci 2009, 326, 322.
10. Bowen, W. R.; Cheng, S. Y.; Doneva, T. A.; Oatley, D. L. J Membr Sci 2005, 250, 1.
11. Bowen, W. R.; Doneva, T. A.; Yin, H. B. J Membr Sci 2002, 206, 417.
12. Shen, L.-Q.; Xu, Z.-K.; Liu, Z.-M.; Xu, Y.-Y. J Membr Sci 2003, 218, 279.
13. Pham, V. A.; Santerre, J. P.; Matsuura, T.; Narbaitz, R. M. J Appl Polym Sci 1999, 73, 1363.
14. Ho, J. Y.; Matsuura, T.; Santerre, J. P. J Biomater Sci Polym Ed 2000, 11, 1085.
15. Rana, D.; Matsuura, T.; Narbaitz, R. M.; Feng, C. J Membr Sci 2005, 249, 103.
16. Rana, D.; Matsuura, T.; Narbaitz, R. M. J Membr Sci 2006, 282, 205.
17. Nguyen, A. H.; Narbaitz, R. M.; Matsuura, T. J Environ Eng 2007, 133, 515.
18. Garand-Sheridan, A.-M. M. Sc. Thesis, University of Ottawa, Ottawa, ON, 2008.
19. Dang, H. T.; Narbaitz, R. M.; Matsuura, T.; Khulbe, K. C. Water Qual Res J Canada 2006, 41, 84.
20. Sivakumar, M.; Susithra, L.; Mohan, D. R.; Rangarajan, R. J Macromol Sci Pure Appl Chem 2006, 43, 1541.
21. Singh, S.; Khulbe, K. C.; Matsuura, T.; Ramamurthy, P. J Membr Sci 1998, 142, 111.
22. Mulder, M. Basic Principles of Membrane Technology; Kluwer Academic: Dordrecht, The Netherlands, 1996.
23. Wan, L.-S.; Xu, Z.-K.; Huang, X.-J.; Che, A.-F.; Wang, Z.-G. J Membr Sci 2006, 277, 157.
24. Khayet, M.; Matsuura, T. Desalination 2002, 148, 31.
25. Khayet, M. Appl Surf Sci 2004, 238, 269.
26. Chen, S.-H.; Lioua, R.-M.; Hsu, C.-S.; Chang, D.-J.; Yu, K.-C.; Chang, C.-Y. J Membr Sci 2001, 193, 59.
27. Sun, H.; Liu, S.; Gea, B.; Xing, L.; Chen, H. J Membr Sci 2007, 295, 2.
28. Raguime, J. A.; Arthanareeswaran, G.; Thanikaivelan, P.; Mohan, D.; Raajenthiren, M. J Appl Polym Sci 2006, 104, 3042.
29. Kim, I. C.; Yun, H. G.; Lee, K. H. J Membr Sci 2002, 199, 75.
30. Zhu, L.-P.; Xu, L.; Zhu, B.-K.; Feng, Y.-X.; Xu, Y.-Y. J Membr Sci 2007, 294, 196.